2. McLennan, S. M., Taylor, S. R. and Kroner, A., Geochemical evolution of Archean shales from South Africa. I. The Swaziland and Pongola Supergroups. *Precambrian Res.*, 1983, **22**, 93–124.
3. Chaudhuri, S. and Cullers, R. L., The distribution of rare earth elements in deeply buried Gulf coast sediments. *Chem. Geol.*, 1979, **24**, 327–338.
4. Nance, W. B. and Taylor, S. R., Rare earth patterns and crustal evolution 1: Australian post-Archean sedimentary rocks. *Geochim. Cosmochim. Acta*, 1976, **40**, 1539–1551.
5. McLennan, S. M. and Taylor, S. R., Geochemical constraints on the growth of the continental crust. *J. Geol.*, 1982, **90**, 347–361.
6. Naqvi, S. M. and Hussain, S. M., Petrochemistry of early Precambrian metasediments from the central part of the Chitradurg Schist Belt, Mysore, India. *Chem. Geol.*, 1972, **10**, 109–135.
7. Wronkiewicz, D. J. and Condie, K. C., Geochemistry and provenance of sediments from the Pongola Supergroup, South Africa: Evidence for a 3.0 Ga old continental craton. *Geochim. Cosmochim. Acta*, 1989, **53**, 1537–1549.
8. Condie, K. C., Chemical composition and evolution of the upper continental crust: Contrasting results from surface samples and shales. *Chem. Geol.*, 1993, **104**, 1–37.
9. Bhat, M. I. and Ghosh, S. K., Geochemistry of the 2.51 Ga old Rampur group pelites, western Himalayas: Implications for their provenance and weathering. *Precambrian. Res.*, 2001, **108**, 1–16.
10. Valdiya, K. S., *Geology of Kumaun Lesser Himalaya*, Wadia Institute of Himalayan, Geology, Dehradun, 1980.
11. Valdiya, K. S., Simla Slates, the precambrian flysch of the Lesser Himalaya: Its turbidites, sedimentary structures and paleocurrents. *Geol. Soc. Am. Bull.*, 1970, **81**, 451–468.
12. Ranga Rao, A., Traverses in the Himalaya of Uttar Pradesh. *Misc. Publ. Geol. Surv. India*, 1972, **15**, 31–44.
13. Rupke, J., Stratigraphic and structural evolution of the Kumaun Lesser Himalaya. *Sediment. Geol.*, 1974, **11**, 81–265.
14. Crawford, A. R., The Indus Suture line, the Himalaya, Tibet and Gondwanaland. *Geol. Mag.*, 1974, **111**, 369–383.
15. Tripathi, J. K. and Rajamani, V., Geochemistry of the loessic sediments on Delhi ridge, eastern Thar desert, Rajasthan: Implications for exogenic processes. *Chem. Geol.*, 1999, **155**, 265–278.
16. Cullers, R. L., The controls on the major- and trace-element evolution of shales, siltstones, and sandstones of Ordovician to Tertiary age in the Wet Mountains region, Colorado, USA. *Chem. Geol.*, 1995, **123**, 107–131.
17. Nesbitt, H. W., Markovics, G. and Price, R. C., Chemical processes affecting alkalies and alkaline earths during continental weathering. *Geochim. Cosmochim. Acta*, 1980, **44**, 1659–1666.
18. Cox, R., Low, D. R. and Cullers, R. L., The influence of sediment recycling and basement composition on evolution of mudrock chemistry in the southwestern United States. *Geochim. Cosmochim. Acta*, 1995, **59**, 2919–2940.
19. Nesbitt, H. W. and Young, G. M., Early Proterozoic climates and plate motions inferred from major element chemistry of lutites. *Nature*, 1982, **299**, 715–717.
20. Gu, X. X., Liu, J. M., Zheng, M. H., Tang, J. X. and Qi, L., Provenance and tectonic setting of the Proterozoic turbidities in Hunan, South China: Geochemical evidence. *J. Sediment. Res.*, 2002, **72**, 393–407.
21. Singh, P. and Rajamani, V., REE geochemistry of recent clastic sediments from the Kaveri floodplains, southern India: Implications to source area weathering and sedimentary processes. *Geochim. Cosmochim. Acta*, 2001, **65**, 3093–3108.
22. Nesbitt, H. W. and Young, G. M., Prediction of some weathering trends of plutonic and volcanic rocks based on thermodynamics and kinetic considerations. *Geochim. Cosmochim. Acta*, 1984, **48**, 1523–1534.
23. McLennan, S. M., Hemming, S., McDaniel, D. K. and Hanson, G. N., Geochemical approaches to sedimentation, provenance, and tectonics. *Geol. Soc. Am. Spl. Pap.*, 1993, **284**, 21–40.
24. Yanjing, C. and Yongchao, Z., Geochemical characteristics and evolution of REE in the early Precambrian sediments: Evidence from the southern margin of the North China craton. *Episodes*, 1997, **20**, 109–116.
25. Condie, K. C., Another look at rare earth elements in shales. *Geochim. Cosmochim. Acta*, 1991, **55**, 2527–2531.
26. Gopalan, K., Macdougall, J. D., Roy, A. B. and Murali, A. V., Sm–Nd evidence for 3.3 Ga old rocks in Rajasthan, northwestern India. *Precambrian Res.*, 1990, **48**, 287–297.
27. Wiedenbeck, M., Goswami, J. N. and Roy, A. B., Stabilization of the Aravalli craton of northwestern India at 2.5 Ga: An ion microprobe zircon study. *Chem. Geol.*, 1996, **129**, 325–340.
28. Mondal, M. E. A., Goswami, J. N., Deomurari, M. P. and Sharma, K. K., Ion microprobe $^{207}Pb/^{206}Pb$ ages of zircons from the Bundelkhand massif, northern India: Implications for crustal evolution of the Bundelkhand–Aravalli Protocontinent. *Precambrian Res.*, 2002, **117**, 85–100.
29. Ahmad, T. and Tarney, J., Geochemistry and petrogenesis of late Archean Aravalli volcanics, basement enclaves and granitoids, Rajasthan. *Precambrian Res.*, 1994, **65**, 1–23.
30. Sun, S.-S. and McDonough, W. F., Chemical and isotopic systematics of oceanic basalts: implications for mantle composition and processes. In *Magmatism in the Ocean Basins* (eds Saunder, A. D. and Norry, M. J.), Geol. Soc. London. Spl. Pub., 1989, vol. 42, pp. 313–345.

ACKNOWLEDGEMENTS. I thank the Chairman, Department of Geology, Aligarh Muslim University, Aligarh for providing necessary facilities. I am grateful to Prof. V. Rajamani, School of Environmental Sciences, JNU, New Delhi for accepting me as a Summer Research Fellow at JNU. I also thank Drs J. Tripathi, P. Kamal, Meenal Mishra, Sudesh and Mr Rajneesh, JNU for co-operation and suggestions. I also thank the Indian Academy of Sciences, Bangalore for providing me financial assistance by granting me the Summer Research Fellowship.

Received 12 February 2004; revised accepted 24 February 2005

Analysis of gravity and magnetic anomalies over Lonar lake, India: An impact crater in a basalt province

R. P. Rajasekhar and D. C. Mishra*

National Geophysical Research Institute, Hyderabad 500 007, India

The amplitude and circular/semi-circular nature of gravity and magnetic anomalies of 2.5 mGal and 550 nT respectively, in the case of Lonar lake are similar to those reported over impact craters. Analysis of these anomalies suggests that the impact has modified the magnetization vector and density of the country rock (Deccan trap) up to about 500–600 m below the surface with a brecciated part of about 135 m of bulk density of 2.60 g/cm^3 and fragmented layer of about 150 m of bulk density 2.7 g/cm^3 with induced magnetization.

*For correspondence. (e-mail: dcm_ngri@yahoo.co.in)

The affected part depth-wise is approximately 0.3–0.35 times the diameter of the crater, as is found in the case of impact craters the world over. The impact has remagnetized this region in the present-day earth's magnetic field, demagnetizing the remanent magnetization of the Deccan trap. This implies that the temperature on impact must have been raised above 550°C corresponding to Curie point of magnetite. Part of the brecciated zone showing very high susceptibility of about 4.0×10^{-3} SI units, suggests concentration of magnetite in this part which may represent parts of meteorite embedded there. This approach may help in the analysis of magnetic and gravity fields due to impact craters of celestial bodies with exposed trap rocks, such as moon, Mars, etc.

LONAR lake (19°58′N; 76°31′E) in Buldhana district, Maharashtra, India (Figure 1) is a circular lake occupied by saline water. It occurs in the Deccan trap covered region and is almost circular with longest and shortest diameters as 1875 m and 1787 m respectively[1], with raised rim of about 30 m and depth of 135 m. The inner and outer rims of the crater coincide approximately with the 480 m and 580 m elevation contours respectively. It is presently filled by water and is therefore inaccessible on ground. Deccan trap originated due to eruption from Reunion plume[2] at about 65 Ma. Based on detailed geological investigations and drilling results, it was suggested that it represents a meteorite impact crater (A. Dube and S. Sen Gupta, unpublished report, GSI, 1984)[3–6], which according to fission track dating took place about 50,000 years ago. This is the only impact crater in basaltic rocks in the world. However, due to its occurrence in the Deccan trap covered region, there has always been a doubt about its volcanic origin[7,8], as several circular volcanic plugs exposed at different places have been reported from this region[9]. Due to erosion, circular lakes could be created over such volcanic plugs, specially over those that are less resistive to erosion compared to surrounding rocks.

Geophysical methods, specially gravity and magnetic methods have been found to be extremely useful to delineate the sites and other details of impact craters the world over[10]. A circular bowl-shaped negative anomaly is observed over simple craters (diameter up to 4 km on the earth). The amplitude of negative gravity anomaly associated with impact craters increases with the crater diameter[10]. The general character of magnetic anomalies associated with impact craters is more complex than gravity signature due to greater variation in magnetic properties of rocks and direction of magnetization. Petrographic and petrochemical studies have provided details of basalt occurring around the crater and its shocked facies have already been described by earlier workers[11]. The Lonar crater and its environs exhibit six flows of Deccan trap basalt. Based on petrochemistry, it is interpreted that the country rock prior to the extraterrestrial impact, was slightly over-saturated tholeiitic basalt belonging to a tectonic setting of normal continental active shield volcano[11]. The basalt from this area had a distinct chemical signature, which differed from the mean Deccan basalt in respect of iron, magnesia and total alkali content showing relatively high magnesia[11].

Meteorite impacts modify the gravity and the magnetic field at the site of impact, which after the impact shows different signatures compared to the surrounding rocks. This is specially true about the magnetic field in a basalt province, as the impact will raise the temperature beyond Curie point of magnetite (550–600°C) and remagnetize it in present-day earth's magnetic field. This process modifies the remanent magnetization of igneous provinces corresponding to the period they intruded/formed initially. We, therefore, investigated the gravity and magnetic fields observed over Lonar lake. The gravity and magnetic anomalies of Lonar lake were obtained using a underwater gravimeter and a vertical intensity magnetometer and a suitable boat[4,8,12]. These observations provided almost circular gravity and magnetic anomalies over the lake of almost –2.25 mGal and 550 nT respectively. The terrain-corrected gravity anomaly[4,8] is reproduced in Figure 2, which shows a circular gravity low

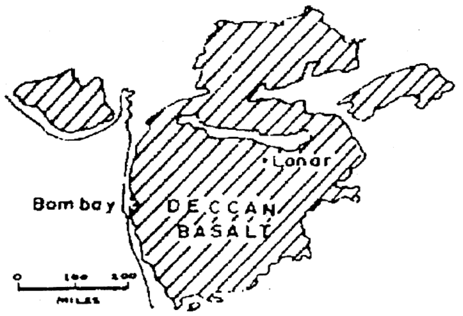

Figure 1. Location map of Lonar lake.

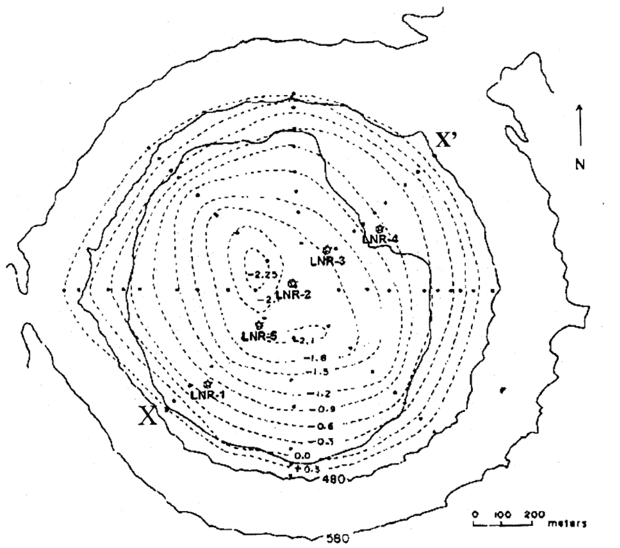

Figure 2. Gravity anomaly with elevation contours (solid lines) superimposed over it. 480 m and 580 m represent the inner and outer rim of the crater[4].

with +0.3 mGal contour almost coinciding with 480 m elevation contour which defines the inner rim of the crater. Circular gravity and magnetic anomalies are observed in both cases of impact craters and in some cases of volcanic plugs, but their amplitudes and signs differ considerably with a few mGal (< 10 mGal) negative gravity anomalies reported for impact craters[10] and 60–80 mGal anomaly over volcanic plugs, specially those reported from the Deccan trap[13]. Magnetic anomalies observed over volcanic plugs, of Deccan trap activity are also of higher order (800–1000 nT) compared to that observed in the present case of the Lonar lake[13]. Further, the former shows negative magnetic anomalies, implying magnetic lows due to remanent magnetization corresponding to Deccan trap activity[13], while the latter provides a magnetic high corresponding to vertical component of the present-day earth's magnetic field indicating remagnetization after impact. The higher amplitude of gravity and magnetic anomalies due to volcanic plugs compared to those due to impact craters, can be attributed to the depth extent of volcanic plugs and higher contrasts in the physical parameters, viz. density and susceptibility, which produce these anomalies. The nature and amplitude of gravity and magnetic anomalies recorded over Lonar lake, therefore, tentatively suggest that it represents an impact crater, which can be confirmed from modelling of the sources causing these anomalies.

Figure 3 *a* shows schematic section of Lonar crater and geology based on surface exposures and diamond drill holes[3] LNR1, LNR2, LNR3. Figure 3 *b* shows gravity and magnetic anomalies along a SW–NE profile *XX′* (Figure 2), which are modelled for a cross-section given at the bottom of the figure. The initial cross-section is made based on information from five boreholes[3,8] up to 300–400 m shown along this profile (LNR1–LNR5). The initial model is modified by computing and comparing the computed and the observed gravity fields. The gravity and magnetic fields were computed using 2.5-dimensional bodies, implying limited strike direction and modified using generalized inversion scheme[14]. The densities of these layers are assigned from measurements in the laboratory of samples from bore holes[8] and density logs from bore holes in different parts of the exposed Deccan trap[13,15] and reported density of Deccan trap in general. Though these bore holes[13,15] are away from the Lonar lake, while considering the bulk density of the Deccan trap, these values can be considered in a general manner. It basically shows three layers corresponding to (1) silt layer in the lake of bulk density 2.0 g/cm^3, (2) brecciated zone of bulk density 2.60 g/cm^3 and (iii) high density fragmented rocks of density 2.7 g/cm^3. The surrounding solid basalt can be assigned a bulk density 2.75 g/cm^3 (Figure 3 *b*), as suggested by previous workers for unweathered massive Deccan basalt[3,13]. The layer (3) relates to high density fragmented rocks, since after the impact these rocks being heavier fall first and occupy the bottom of the crater, with brecciated low density parts over them. The magnetic field from this cross-section is computed by assigning susceptibilities similar to those reported for the Deccan trap in adjoining regions[16,17]. However, when the same susceptibility distribution could not produce the observed magnetic field, a dyke type of body numbered as (4) in Figure 3 *b* (thin line) is introduced, which shows the same density as layers (2) and (3) but divides them into three parts of different susceptibilities. The model shows a high susceptibility rock/body ((4), Figure 3 *b*) under the magnetic 'high' compared to those surrounding it, which provides a good match between observed and the computed fields. In general, the changes in density are quite subtle compared to susceptibility and therefore, it is quite often possible that density, specially bulk density, may remain the same while susceptibility within the same rock type, specially in case of basalts, changes considerably. In fact, this property of the

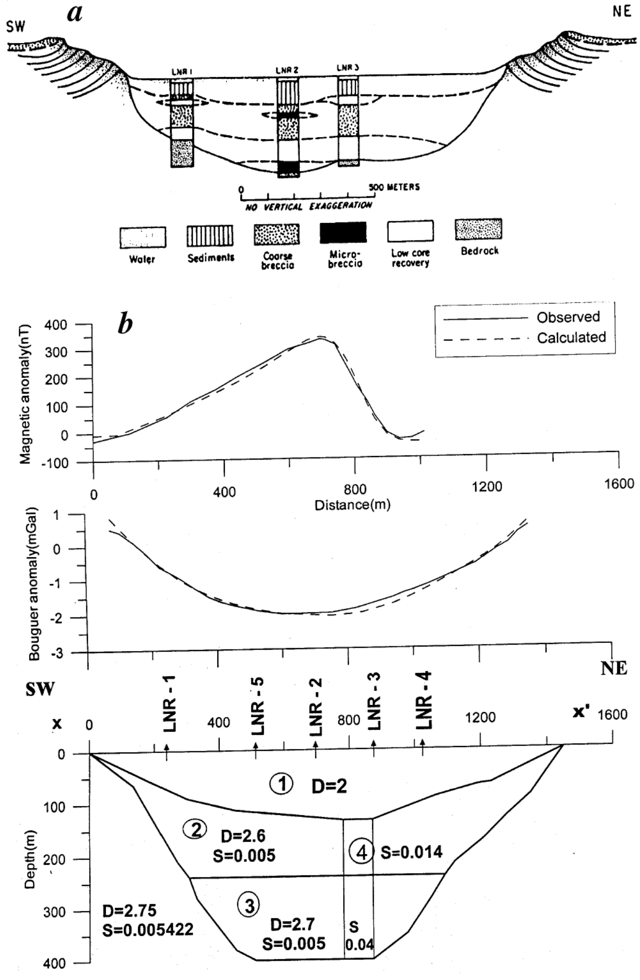

Figure 3. *a*, Schematic section of Lonar crater and geology based on surface exposures and diamond drill holes[3]. ***b***, A SW–NE magnetic and gravity profile (XX′, Figure 2) across Lonar lake and subsurface layers which produce the observed fields for density (*D*, g/cm^3) and susceptibility (*S*, SI units) given inside the layers. Three layers, viz. 1, silt in the lake; 2, brecciated part, and 3, fragmented basalt are seen. A body (4) of high susceptibility is introduced below the observed magnetic high, which divides the bodies (2) and (3) of different susceptibilities to match the observed magnetic field. LNR-1 to LNR-5 represent location of drill holes along the profile.

Deccan trap explains the sudden variations in magnetic field in magnetic surveys over the Deccan trap, while the gravity field shows a smoothly varying field.

Modelling along the profile XX' is based on a scheme for a 2.5-dimensional body. However, gravity anomaly (Figure 3 *b*) suggests that it is a truly three-dimensional body of basinal type with major density contrast along the interface separating the brecciated part and the unaffected Deccan basalt. We therefore employed the harmonic inversion scheme[18,19] to model the three-dimensional configuration of parts of Deccan basalt affected by this impact. This method states that the Fourier transform of the observed field is related to the transform of the causative body through a filter function whose inverse transform provides the configuration of the source.

$$g(f) = \sum_{f=-n/2}^{n/2} 2\pi G\rho[\exp(-2\pi f z_0/\lambda)]Z(f), \tag{1}$$

where $g(f)$ is the transform of the observed field; n is the number of observations/digitized data along a profile; f the frequencies equal to $\pm 1, \pm 2, \ldots, \pm n/2$, when n is even and $\pm 1, 2, \ldots, \pm (n-1)/2$ when n is odd; G the gravitational constant; ρ the density contrast across the interface; z_0 the average depth of the relief; λ the wavelength equal to length of the data = n* data spacing and $Z(f)$ the transform of the shape of the body known as shape factor[20].

In case ρ and z_0 can be constrained from field observations/measurements, $Z(f)$ can be uniquely determined from eq. (1) and its inverse transform provides depth at every point of observation, which can be contoured in the form of a bowl structure. Equation (1) can be formulated for two-dimensional data with frequencies k and m along the x and y axes, such that $f = (k^2 + m^2)^{1/2}$.

In the present case the volumetric density of layers (1) and (2) provides a bulk density of approximately 2.51 g/cm^3,

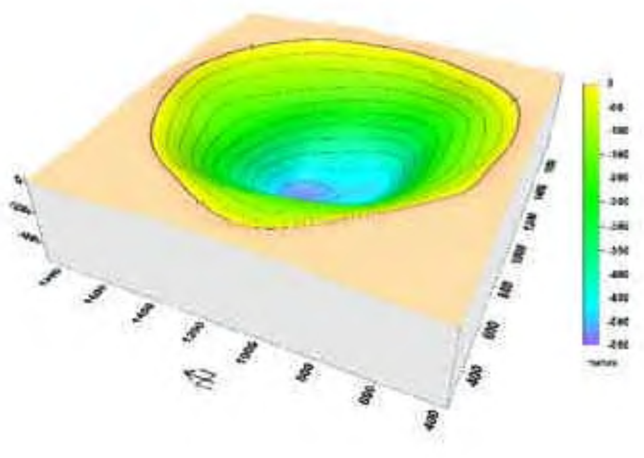

Figure 4. A 3D view of affected part of Deccan trap due to impact computed from gravity anomaly (Figure 2) based on harmonic inversion as given in eq. (1). It suggests a maximum depth of 500 m of affected part due to impact.

implying a density contrast of 0.24 g/cm^3 with respect to layer (3). With this density contrast as ρ and $z_0 = 0$, eq. (1) is used to transform the digital data of gravity anomaly (Figure 2) in a three-dimensional model as given in Figure 4. It provides a basinal structure with zero contour, almost coinciding with zero contour of gravity anomaly (Figure 1) and suggests maximum depth of 500 m to the unaffected basalt. This depth is with reference to 480 m of elevation contour, which defines the inner rim of the crater.

Modelling of gravity and magnetic anomalies in the previous section suggests that an impact crater of approximate dimension 1875×1787 m^2 affects up to a depth of 450–500 m from the inner rim of the crater. This amounts to 550–650 m from the surface, which is almost 0.3–0.35 times the surface extent, as is generally found the world over. It also suggests that the layers are magnetized in present-day earth's magnetic field, thereby indicating that due to impact and related rise in temperature, the original magnetic field of the Deccan trap is modified, which in unaffected parts corresponds to remanant magnetization in the southern hemisphere, where India was located during eruption of these rocks[17]. The body (4) (Figure 3 *b*) with high susceptibility compared to the surrounding rocks suggests concentration of magnetite in this part, which may represent fragments of meteorite embedded in the brecciated part of the Lonar lake as the ejecta cloud later settled along with the rock chips. Meteorites are usually more mafic compared to normal basalt. The variations in density being more subtle, it cannot be differentiated in the present computation and is included in the bulk density adopted for the computation of gravity field. The higher bulk density of the fragmented part (layer 3) also suggests that it may be containing some high-density rocks at places, which may represent parts of the meteorite. It may be mentioned here that a satellite crater about 300 m north of main crater[3] does not show any well-defined magnetic anomaly[8]. Instead it shows sharply varying magnetic anomalies typical of those observed over the Deccan trap. This suggests that the magnetic field in the region of the main Lonar crater, which shows a pair of well-defined magnetic anomalies with a magnetic low toward north as expected in the present-day earth magnetic field in this region, is caused due to induced magnetization. This shows that quantitative modelling of gravity and magnetic anomalies, specially the latter, of impact craters in basalt provinces provides significant information. Most celestial bodies being composed of basaltic rocks, the satellite gravity and magnetic field recorded over Mars and moon can be analysed in this manner, to differentiate volcanic plugs and impact craters and delineate their subsurface structures and effects.

1. La Touche, T. H. D. and Christie, W. A. K., The geology of the Lonar lake. *Rec. Geol. Surv. India*, 1912, **14**, 266–289.
2. White, R. S. and McKenzie, D. P., Magnetism at rift zones. The generation of volcanic continental margins and flood basalt. *J. Geophys. Res.*, 1989, **94**, 7685–7729.

3. Fredriksson, K., Dube, A., Milton, D. J. and Balasundaram, M. S., Lonar lake, India: An impact crater in basalt. *Science*, 1973, **180**, 862–864.
4. Fudali, R. F., Milton, D. J., Fredriksson, K. and Dube, A., Morphology of the Lonar crater, India: Companions and implications. *The Moon and the Planets*, 1980, **23**, 493–515.
5. Nayak, V. K., Glassy objects (impact glasses?) A possible new evidence for meteoritic origin of Lonar crater, Maharashtra state, India. *Earth Planet. Sci. Lett.*, 1972, **14**, 1–6.
6. La Fond, E. C. and Dietz, R. S., Lonar crater, India, a meteorite crater? *Meteoritics*, 1964, **2**, 111–116.
7. Bucher, W. A., Crypto explosion structure caused from without or within the earth 'Astrobleme or Geoleme'. *Am. J. Sci.*, 1963, **261**, 577–649.
8. Subrahmanyam, B., Lonar crater, India: A Crypto-volcanic origin. *J. Geol. Soc. India*, 1985, **26**, 326–335.
9. Basu, A. R., Renne, P. R., Dasgupta, D. K., Teichman, F. and Poreda, R. J., Early and late alkali igneous pulses and a high-^{3}He plume origin for the Deccan flood basalts. *Science*, 1993, **261**, 902–906.
10. Pilkington, M. and Grieve, R. A. F., The geophysical signature of terrestrial impact craters. *Rev. Geophys.*, 1992, **30**, 161–181.
11. Ghosh, S. and Bhaduri, S. K., Petrography and petrochemistry of impact melts from Lonar lake, Buldana district, Maharashtra, India. *Indian Miner.*, 2003, **57**, 1–26.
12. Fudali, R. F. and Subrahmanyam, B., *Gravity Reconnaissance at Lonar Crater, Maharashtra*, GSI Special Publication Series No. 2 1983, 1978, vol. 1, pp. 83–87.
13. Chandrasekhar, D. V., Mishra, D. C., Rao, G. V. S. P. and Rao, J. M., Gravity and magnetic signatures of volcanic plugs related to Deccan volcanism in Saurashtra, India and their physical and geochemical properties. *Earth Planet. Sci. Lett.*, 2002, **201**, 277–292.
14. Webring, M., SAKI: A Fortran program for generalised inversion of gravity and magnetic profiles. U.S.G.S. Open File Report, 1986, pp. 85–122.
15. Gupta, H. K. *et al.*, Bore hole investigations in the surface rupture zone of the 1993 Latur SCR earthquake, Maharastra, India: Overview of results. *Mem. Geol. Soc. India*, 2003, **54**, 1–22.
16. Rao, G. V. S. P. and Bhalla, M. S., Lonar lake: Paleomagnetic evidence of shock origin. *Geophys. J. R. Astron. Soc.*, 1984, **77**, 847–862.
17. Vandamme, D., Courtillot, V., Besse, J. and Montigny, R., Paleomagnetism and age determinations of the Deccan traps (India): Results of a Nagpur–Bombay traverse and review of earlier work. *Rev. Geophys.*, 1991, **29**, 159–190.
18. Hahn, A., Kind, E. G. and Mishra, D. C., Depth estimation of magnetic sources due to Fourier amplitude spectra. *Geophys. Prospect.*, 1976, **24**, 287–308.
19. Mishra, D. C. and Pederson, L. B., Statistical analysis of potential fields from subsurface reliefs. *Geoexploration*, 1982, **19**, 247–265.
20. Spector, A. and Grant, F. S., Statistical models for interpreting aero magnetic data. *Geophysics*, 1970, **35**, 293–302.

ACKNOWLEDGEMENTS. We thank Director, NGRI for his permission to publish this work. We thank CSIR, for Emeritus Scientist Scheme under which this work was carried out.

Received 23 March 2004; revised accepted 22 February 2005

Effect of Tibetan spring snow on the Indian summer monsoon circulation and associated rainfall

M. S. Shekhar* and S. K. Dash

Centre for Atmospheric Sciences, Indian Institute of Technology Delhi, Hauz Khas, New Delhi 110 016, India

In this communication, the effect of Tibetan snowfall in the month of April on the Indian summer monsoon circulation and associated seasonal rainfall has been examined using the Regional Climate Model version 3. This model has been integrated at 55km horizontal resolution from April to September in each of the years from 1993 to 1996. NIMBUS-7 SMMR snow depth data have been used as boundary conditions. Sensitivity experiment shows that Tibetan snow results in weak lower level monsoon westerlies and upper level easterlies. Without any initial snow, the sensible heat flux is found to be more, whereas with snow, the latent heat flux is more over the Tibetan region. Results indicate that the Indian Summer Monsoon Rainfall is reduced over entire India and its five homogeneous zones, when 10 cm of snow has been introduced over the Tibetan region in the preceding month of April. Quantitatively, rainfall decreases by 30% for all India, 23% for northwest India, 20% for west central India, 25% for central northeast India, 30% for northeast India and 15% for south peninsular India.

THE Tibetan Plateau, known as the Roof of the World, has been recognized as the heat source/sink in summer/winter for the monsoon circulation over India. In the literature[1–4] it has been mentioned as one of the most important factors for the generation and maintenance of Indian summer monsoon circulation and rainfall. During summer, the Tibetan Plateau due to its high elevation receives a large amount of solar radiation, which effectively heats the mountain surface creating a strong heat contrast at the mid-tropospheric level. This causes a heat low near the surface and anticyclone (Tibetan High) above[2,3]. The sensible heat as well as latent heat flux released over the Tibetan Plateau drives the Asian monsoon circulation and strongly influences global circulation patterns[2]. Results[4] also show that the latent heating plays a more important role than the sensible heating for the maintenance of the Tibetan High. There is a sharp contrast between the western and eastern plateau in terms of precipitation and moisture distribution. Studies[2,3] show that the sensible heat flux is extremely large over arid western Tibetan Plateau during June compared to the eastern side. On the other hand, in the eastern side of the Tibetan Plateau, the latent heat flux is more, so much so that the eastern plateau is described[5] as a huge chimney funnelling water vapour from the lower to the upper

*For correspondence. (e-mail: shekar@cas.iitd.ernet.in)